IEEE Photonics Journal
An IEEE Photonics Society Publication

Open Access

Development of Nanoengineered Thulium-Doped Fiber Laser With Low Threshold Pump Power and Tunable Operating Wavelength

Volume 7, Number 1, February 2015

M. C. Paul
A. Dhar
S. Das
A. A. Latiff
M. T. Ahmad
S. W. Harun

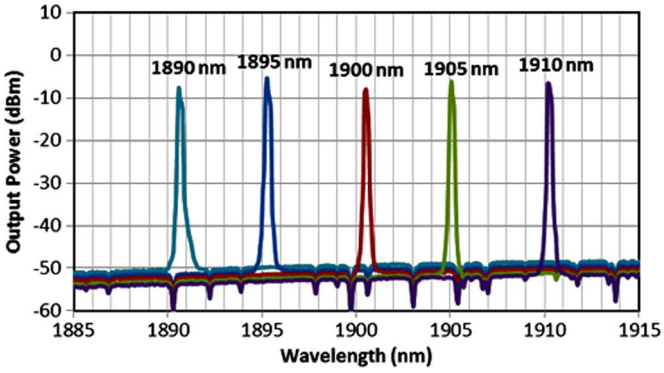

DOI: 10.1109/JPHOT.2015.2399357
1943-0655

IEEE photonics SOCIETY

IEEE

Development of Nanoengineered Thulium-Doped Fiber Laser With Low Threshold Pump Power and Tunable Operating Wavelength

M. C. Paul,[1] A. Dhar,[1] S. Das,[1] A. A. Latiff,[2,3] M. T. Ahmad,[3] and S. W. Harun[2,4]

[1]Fiber Optics and Photonics Division, CSIR-Central Glass and Ceramic Research Institute, Kolkatta 700032, India
[2]Photonics Research Center, University of Malaya, 50603 Kuala Lumpur, Malaysia
[3]Faculty of Electronic and Computer Engineering, Universiti Teknikal Malaysia Melaka, 76100 Melaka, Malaysia
[4]Department of Electrical Engineering, Faculty of Engineering, University of Malaya, 50603 Kuala Lumpur, Malaysia

DOI: 10.1109/JPHOT.2015.2399357

Manuscript received December 25, 2014; revised January 25, 2015; accepted January 28, 2015. Date of publication February 2, 2015; date of current version February 19, 2015. This work was supported by Ministry of Education High Impact Research under Grant D000009-16001. Corresponding authors: S. W. Harun and M. C. Paul (e-mail: swharun@um.edu.my; paulmukul@hotmail.com).

Abstract: A tunable and low-threshold thulium (Tm)-doped fiber (TDF) laser is demonstrated using a new silica-based nanoengineered TDF in a linear configuration, in conjunction with 1552-nm pumping. The TDF used in these experiments had a Tm-doped nanoengineering yttrium–alumina–silica glass core with a diameter of 13.43 μm and 0.21 NA, which is surrounded by a pure silica inner cladding with normal acrylate polymer resin coating. The nanoengineered TDF was fabricated using a modified chemical vapor deposition (MCVD) process, in conjunction with a solution-doping technique. The fabricated fiber shows an absorption loss of 165 dB/m at 793 nm. A maximum lasing slope efficiency of 26.2% was obtained at a 1910-nm wavelength using the fabricated fiber with an optimum length of 5 m. The maximum output power of 138 mW was achieved at the maximum pump power of 1100 mW. The lowest pump power threshold of 693 mW for a 1552-nm wavelength was obtained at a TDF length of 7 m. The operating wavelength of the laser could be continuously tuned from 1890 to 1910 nm with an optical signal-to-noise ratio better than 43 dB, whereas the slope efficiency of the laser varies from 16.4% to 19.7%.

Index Terms: Nano-engineered glass, Thulium-doped fiber, tunable (Tm)-doped fiber laser (TDFL), silica based TDFL.

1. Introduction

Thulium (Tm)-doped fiber lasers (TDFLs) operating at 1.9–2.1 μm, are emerging as the latest revolution in fiber laser technology [1]–[3]. This is due to the possibility of producing high efficiency, high output power, and retina safe lasers for specific applications associated with this wavelength, such as remote sensing and biomedical applications [4], [5]. Although no laser is completely safe for human eyes, this technology falls under “eye-safer” category, promising several advantages over the traditional 1-μm lasers in industrial and military directed-energy

applications. The permissible power transmission in free space at 2 μm can be several orders of magnitude greater than at 1 μm. Military deployment of laser weapon systems could certainly find wider acceptance if the systems operate at eye-safer wavelengths. Pulsed laser systems may be used either for direct applications such as light detection and ranging (LIDAR) and range finding or for conversion into the mid- and far-IR for military countermeasures, remote sensing, and spectroscopy [6]. Single-frequency systems at 2-μm are of interest for wind shear and turbulence mapping as well as coherent detection. In the medical market, Tm-doped fiber lasers offer a potential alternative to current-generation CW solid-state 2-μm lasers.

To date, many different glass host materials have been used to fabricate Tm^{3+}-doped optical fibers for 2-μm laser operation, including silica and nonsilica glass fibers such as germanate- and tellurite-based types [7], [8]. It is well known that the doping concentration of rare-earth ions in silica fiber is limited due to the intrinsic glass network structure. Various approaches have been developed to increase the ion-doping concentration including co-doping with such oxides as Al_2O_3, B_2O_3, and P_2O_5 and by using nanoparticle technology. The highest doping level in silica glass is limited to approximately 2wt%. Due to the limited Tm^{3+}-doping concentration, the efficiency of Tm^{3+}-doped silica fiber lasers is also limited. Fortunately, the less defined glass network of multicomponent nonsilica glasses permit a higher doping concentration of Tm^{3+} ions, which in turn permits high pump absorption over a relatively short length of active fiber.

In this paper, an efficient and low threshold TDFL is demonstrated using a newly developed Thulium doped fiber (TDF) in conjunction with 1552 nm pumping. In this work, the pumping is implemented using Erbium Ytterbium co-doped fiber laser (EYDFL). It is expected that the lower quantum defect associated with pumping at $\sim$1.5 μm would yield a much higher conversion efficiency than pumping at 0.8 μm. Since the main glass network is silicon dioxide (SiO_2)—the same material as standard silica glass fiber—the doped fiber improves in mechanical strength and shows better compatibility with silica fiber than any other multicomponent glass fibers. This property allows more robust fusion splicing between the active fibers and the standard passive silica fibers.

2. Fabrication and Characterization of Thulium-Doped Nano-Engineering Glass Based Fiber

Doping of Tm_2O_3 into thermally induced phase-separated host of Y_2O_3 within SiO_2-Al_2O_3 with the addition of P_2O_5 was done by the solution doping (SD) technique in combination with modified chemical vapor deposition (MCVD) process. This was followed by a suitable thermal annealing of the fabricated preform. Then, P_2O_5 was incorporated from the vapor phase deposition and other dopants were incorporated by soaking of the phospho silica layer into an alcoholic solution of suitable strength of $TmCl_3$ $6H_2O$, $AlCl_3$ $6H_2O$, and YCl_3 $6H_2O$. In the experiment, the deposition of single porous phospho silica layer was done at a temperature of 1500 °C. Then the temperature was lowered to 1450 °C for the pre-sintering process. All the co-dopants in the solution went into the silica glass matrix during sintering stage after solution soaking process. Next, during collapsing process, the core glass became phase-separated into silica rich and deficient regions that form a glass matrix. After fabricating the fiber preform, thermal annealing was done at 1450–1500 °C for 3 hours at the heating and cooling rates of 20 °C/min. During this step, Tm_2O_3 doped phase-separated nano-particles were created within the core glass matrix. Finally, the structure and composition of nano-particles were evaluated by the electron diffraction and energy dispersive X-ray (EDX) analyses.

Fig. 1 shows the transmission electron microscopy (TEM) image of the core glass matrix together with electron diffraction measurement results on and out of the particles. The EDX spectra show that the phase-separated particles are Tm_2O_3 doped yttria-alumina rich particles embedded within silica glass matrix. The size of the nano-particles is around 5.0–10.0 nm range (bright spots in the TEM image are the phase-separated regions). The EDX spectra also reveal that yttrium and thulium are dominant in phase-separated particles sparse in the non-phase-separated areas. In addition, the intensity of aluminum and yttrium in phase-separated particles is much lower than that in non-phase-separated region. Thus, we can conclude that majority of thulium is

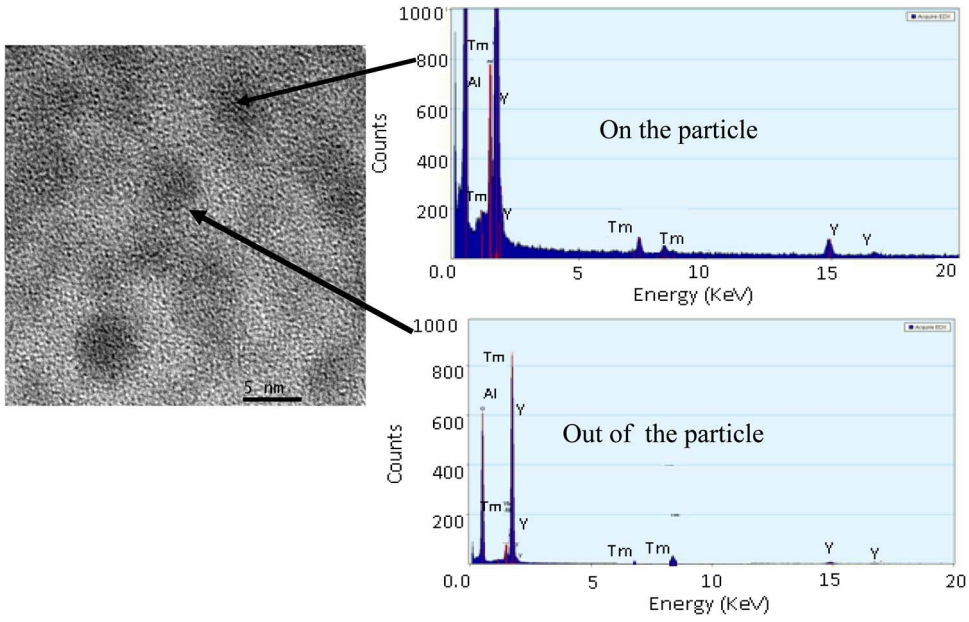

Fig. 1. TEM image and diffraction pattern of the fiber along with EDX analysis taken on and out of the particles.

located in the phase-separated yttria-alumina rich region rather than in non-phase-separated areas. The nature of phase-separated particles was found to be non-crystalline, confirmed by their electron diffraction pattern, shown in the inset of Fig. 1. Diffused scattering in the electron diffraction pattern reveals the amorphous nature of the particles (see a "halo pattern"), since there is no diffraction spot in it.

Here P_2O_5 content in glass accelerates the growth of phase separated particles by heating or thermal perturbation, where P_2O_5 serves as a nucleating agent owing to the higher field strength difference (> 0.31) between Si^{4+} and P^{5+} [9]. The formation of phase-separated nano-particles starts when the ratio of Al:Y reaches $\sim$1.70–1.75 under suitable doping levels of Y_2O_3 and Al_2O_3 [10]. One of the reasons is possibly due to YAS glass undergoing phase-separation once it "enters" the immiscible region.

The average dopant percentages were measured by an electron probe micro analyzer (EPMA) and the distribution profile of different dopants along the diameter of fiber core is shown in Fig. 2. It can be seen that all dopants are distributed uniformly along the entire core where the concentrations of Al_2O_3, Y_2O_3, and Tm_2O_3 are 1.2, 0.4 and 0.4 wt. %, respectively. The amount of P_2O_5 doping is very small. The core and cladding geometry of the fiber was inspected by optical microscope (Olympus BX51) and its cross-section view is shown in the inset of Fig. 2. The measured core and cladding diameters of the fiber are 13.43 μm and 130.70 μm, respectively. Fig. 3 shows the absorption loss curve of the fiber which peaks at around 462 nm, 680 and 793 nm. As shown in the figure, the absorption loss of the fiber at 793 nm wavelength is around 165 dB/m. The refractive index (RI) profile of the fiber preform was measured by preform analyzer as shown in the inset of Fig. 3. It shows an index difference of 0.015 between the core and cladding and thus the numerical aperture of the fiber is estimated to be around 0.21.

3. ASE Characteristics and Laser Configuration

The ASE characteristics of the fabricated TDF is investigated by forward pumping the fiber with a 1552 nm Erbium-Ytterbium co-doped fiber laser (EYDFL) at the maximum output power of 950 mW. This pump wavelength is chosen because it operates at near peak absorption wavelength of Tm ions and high-powered 1.5 μm laser diodes are still relatively new. The ASE

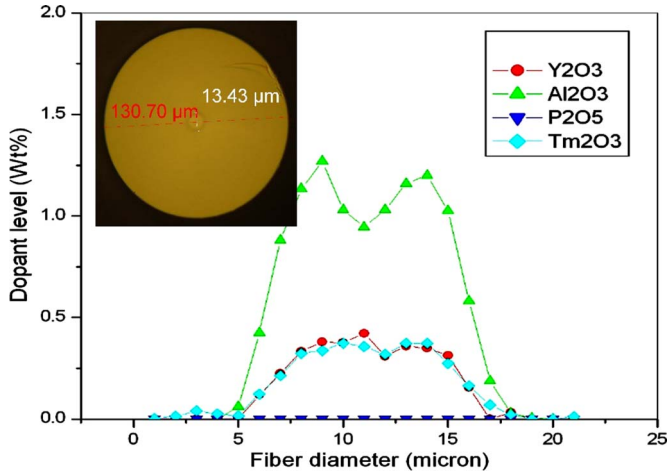

Fig. 2. Distribution of different dopants along the diameter of core region. (Inset) Micro-scopic cross-sectional view of fiber.

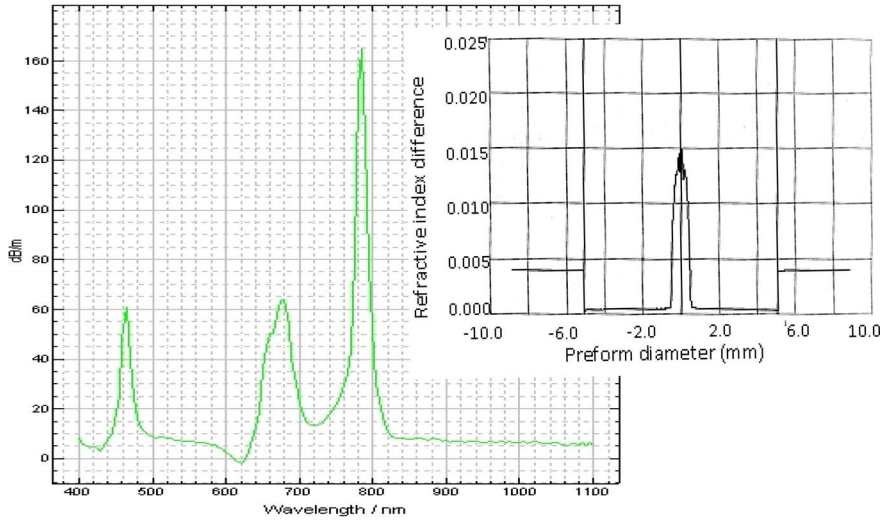

Fig. 3. Spectral attenuation curve of the fabricated TDF. (Inset) Refractive index profile of fiber preform.

emission was investigated for four different fiber lengths ranging from 3 to 8 m using an optical spectrum analyzer (OSA). The output ASE is shown in Fig. 4. As seen in the figure, all spectra show a broadband ASE at 1900-nm region. This is attributed to the 1552 nm pumping, which excites the Tm ion from the ground state to the higher energy levels of $^3F_4$. Then, the Tm ions decay to create a population inversion between $^3F_4$ and $^3H_4$ levels of the Tm ions, which generates spontaneous emission at around 1900-nm region. The ASE power increases with the pump power due to the population inversion, which increases with the rise in pump power. However, the population inversion saturates at the TDF length of around 8 m due to limitation of the available pump power, which is not sufficient to support the excitation of more ions.

The configuration of the proposed TDFL with the fabricated TDF as the gain medium is shown in Fig. 5. A piece of the newly developed silica TDF was pumped by a 1552 nm Erbium-Ytterbium fiber laser via 1550/2000 nm wavelength division multiplexer (WDM). To form a cavity, a tunable fiber Bragg grating (FBG) is used in conjunction with the Fresnel reflection at the output end of the fiber laser. The FBG operates within 1890 nm to 1910 nm with reflectivities of about 90% and

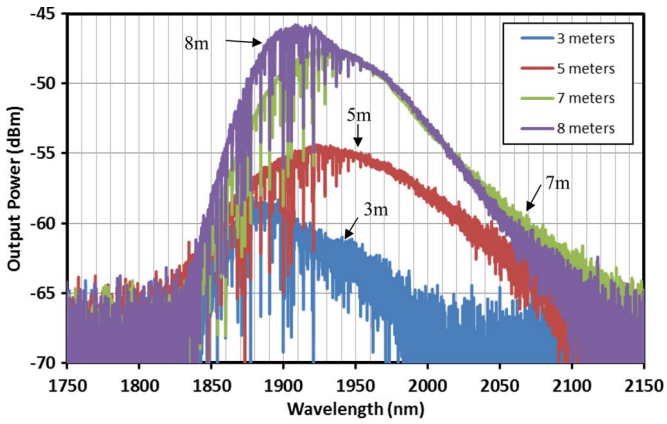

Fig. 4. ASE spectra from the forward pumped TDF at various fiber lengths.

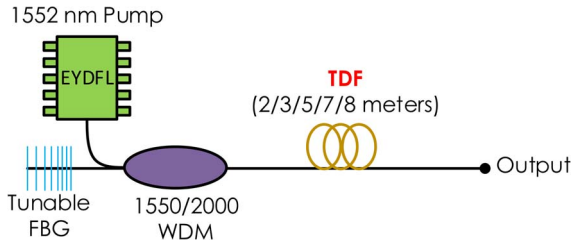

Fig. 5. Configuration of the proposed tunable TDFL.

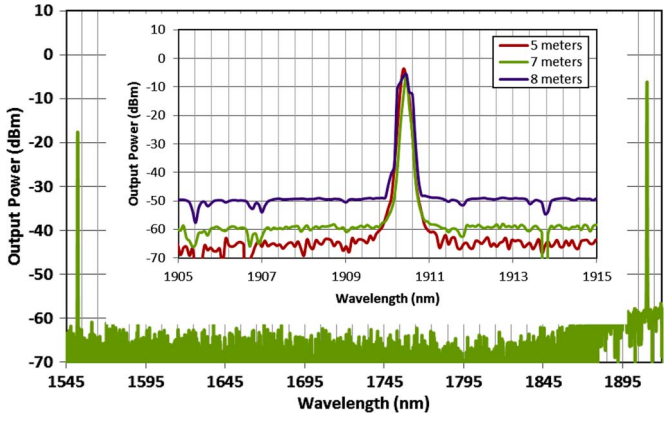

Fig. 6. Output spectrum of the proposed TDFL at 1552 nm pump power of 950 mW. (Inset) Enlarged output spectra at three different TDF lengths.

the corresponding 3 dB spectral width of 0.4 nm. The output spectrum and power of the tunable laser are measured by an OSA and power meter, respectively.

4. Lasing Performances

The lasing performance of the newly developed TDFL is first investigated at FBG wavelength of 1910 nm. Fig. 6 shows the output spectrum of the proposed laser at 1552 nm pump power of 950 mW. As shown in the figure, the laser operates at 1910 nm, which coincides with the FBG's wavelength. The separation between the peak laser power and the residual pump is more than 11 dB. It is also observed that the noise level of the laser drops as the TDF length reduces from

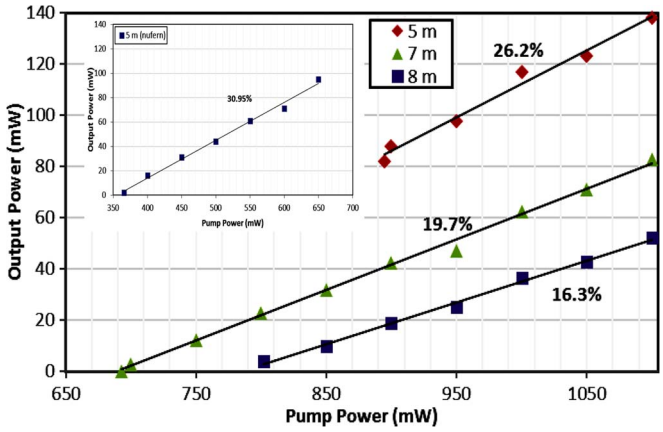

Fig. 7. Lasing characteristic of the fabricated TDFL at three different TDF lengths. (Inset) Lasing characteristic with the commercial TDF.

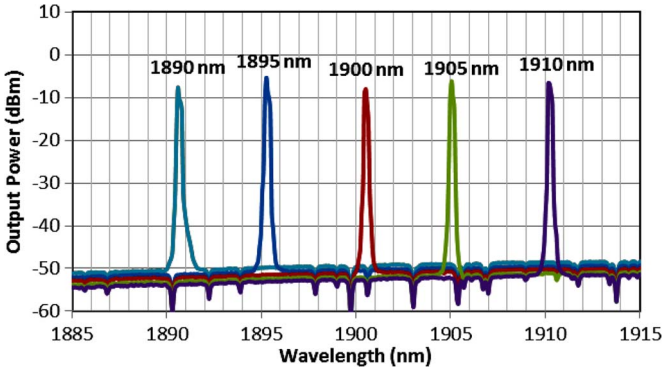

Fig. 8. Output spectra of the tunable TDFL.

8 m to 5 m as shown in the inset of Fig. 6. At TDF length of 5 m, the signal-to-noise ratio is measured at 60 dB. The laser operation was also investigated at TDF lengths of 2 and 3 m, but the pump power threshold needed for lasing was higher than 1100 mW.

Fig. 7 shows the lasing characteristic of the TDFL at three different gain medium lengths. As shown in the figure, the slope efficiencies of the proposed TDFL are 26.2%, 19.7%, and 16.3% at TDF lengths of 5 m, 7 m, and 8 m, respectively. The maximum slope efficiency of 26.2% is obtained at the TDF length of 5 m. The maximum output power of 138 mW is achieved at the pump power of 1100 mW with the optimum length of 5 m. The slope efficiency of the laser drastically decrease as the TBF length decreases to 4 m and below. In addition, both lasing threshold and residual pump will also increase with further reduction of the gain medium length. On the other hand, the pump power threshold for the proposed laser is obtained at around 875 mW, 693 mW, and 802 mW with fiber lengths of 5 m, 7 m, and 8 m, respectively. This is attributed to the population inversion, which is efficient at the optimum TDF length of 7 m and thus a required pump power to initiate lasing is lower. The inset of Fig. 7 shows the lasing characteristic of a TDFL configured with a 5 m long commercial TDF (Nufern) based on the similar setup. This TDFL produces a lasing at 1910 nm with slope efficiency of 31% with a threshold pump power of 365 mW. This shows that our homemade TDFL produces comparable results with the commercial fiber.

A TDFL with a widely tunable output wavelength is important for applications. Here, the wavelength tunability of the proposed TDFL is demonstrated by using spectral controlling of FBG, which is realized by stretching technique. Fig. 8 shows the output spectra measured by an OSA with a spectral resolution of 0.05 nm. In the experiment, the TDF length was fixed at 7 m as this

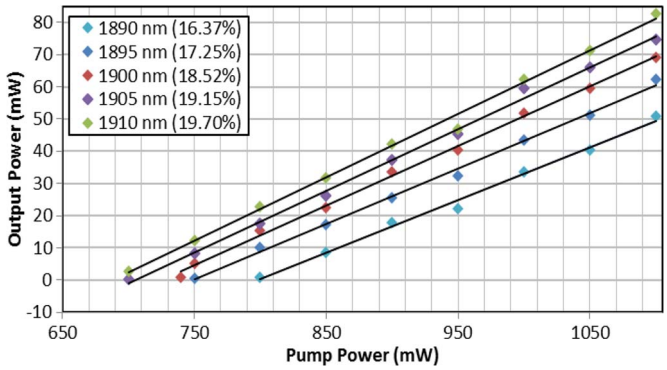

Fig. 9. Lasing characteristics of the tunable TDFL at various operating wavelengths.

length requires the lowest threshold pump power for lasing. As shown in the figure, the operating wavelength of the laser could be continuously tuned from 1890 nm to 1910 nm. The optical signal-to-noise ratio for each spectrum is better than 43 dB. The measured output power characteristic with respect to the operating pump power is shown in Fig. 9 for various operating wavelengths. The slope efficiency of the laser varies from 16.4 to 19.7% as the operating wavelength is tuned from 1890 to 1910 nm. The highest slope efficiency of 19.7% is obtained at 1910 nm with 82.8 mW output power at 1100 mW pump power. The tunability of the laser could be extended to a wider range should another tunable FBG with a wider range is used. The slope efficiency of the tunable laser can also be improved by reducing the insertion loss of the tunable filter. The modal properties of the TDF will be investigated in future work since the multimode character of lasing should affect its the laser performances in term of efficiency, stability, etc. The further optimization of the TDF structure and doped ion compositions are also expected to improve the slope efficiency of the laser.

5. Conclusion

A silica-based nano-engineered TDFL with a low pump power threshold and tunable operating wavelength is demonstrated using a newly fabricated TDF as a gain medium. Doping of Tm_2O_3 into thermally induced phase-separated host was done by the SD technique. The fabricated TDF has a core diameter of 13.43μm, NA of 0.21 and an absorption loss of 165 dB/m at 793 nm. The laser employs a linear configuration with a tunable grating to generate laser with a maximum slope efficiency of 26.2% and TDF length of 5 m. With 7 m long TDF, the laser was achieved at the lowest 1552 nm pump power threshold of 693 mW, while the operating wavelength could be continuously tuned from 1890 nm to 1910 nm. The optical signal-to-noise ratio for each spectrum is better than 43 dB. The slope efficiency of the tunable laser varies from 16.4 to 19.7% at TDF length of 7 m.

Acknowledgement

The authors are thankful to the Director, CGCRI, for his continuous encouragement, guidance, and support in this work.

References

[1] S. D. Jackson and T. A. King, "Theoretical modelling of Tm-doped silica fiber lasers," *J. Lightw. Technol.*, vol. 17, no. 5, pp. 948–956, May 1999.
[2] P. F. Moulton *et al.*, "Tm-doped fiber lasers: Fundamentals and power scaling," *IEEE Sel. Topics Quantum Electron.*, vol. 15, no. 1, pp. 85–92, Jan. 2009.
[3] S. W. Harun *et al.*, "Self-starting harmonic mode-locked thulium-doped fiber laser with carbon nanotubes saturable absorber," *Chin. Phys. Lett.*, vol. 30, no. 9, Sep. 2013, Art. ID. 094204.
[4] N. M. Fried, G. A. Lagoda, N. J. Scott, L.-M. Su, and A. L. Burnett, "Noncontact stimulation of the cavernous nerves in the rat prostate using a tunable wavelength thulium fiber laser," *J. Endourol.*, vol. 22, no. 3, pp. 409–13, Mar. 2008.

[5] R. L. Blackmon, P. B. Irby, and N. M. Fried, "Enhanced thulium fiber laser lithotripsy using micro-pulse train modulation," *J. Biomed. Opt.*, vol. 17, no. 2, Feb. 2012, Art. ID. 028002.
[6] R. J. De Young and N. P. Barnes, "Profiling atmospheric water vapor using a fiber laser lidar system," *Appl. Opt.*, vol. 49, no. 4, 562–567, Feb. 2010.
[7] X. Fan *et al.*, "A 2 μm continuous wave and passively Q-switched fiber laser in thulium-doped germanate glass fibers," *Laser Phys.*, vol. 24, no. 8, Aug. 2014, Art. ID. 085107.
[8] Z.-X. Jia *et al.*, "Supercontinuum generation and lasing in thulium doped tellurite microstructured fibers," *J. Appl. Phys.*, vol. 115, no. 6, Feb. 2014, Art. ID. 063106.
[9] M. C. Paul *et al.*, "Yb_2O_3 doped YAG nano-crystallites in silica based core glass matrix of optical fiber preform," *Mater. Sci. Eng. B*, vol. 175, no. 2, 108–119, 2010.
[10] M. Tomazawa and R. H. Doremus, *Phase Separation in Glass*, Academic, New York, NY, USA, 1979, vol. 17, p. 71.